

Self-Supervised Learning of Visual Servoing for Low-Rigidity Robots Considering Temporal Body Changes

Kento Kawaharazuka¹, Naoaki Kanazawa¹, Kei Okada¹, and Masayuki Inaba¹

Abstract—In this study, we investigate object grasping by visual servoing in a low-rigidity robot. It is difficult for a low-rigidity robot to handle its own body as intended compared to a rigid robot, and calibration between vision and body takes some time. In addition, the robot must constantly adapt to changes in its body, such as the change in camera position and change in joints due to aging. Therefore, we develop a method for a low-rigidity robot to autonomously learn visual servoing of its body. We also develop a mechanism that can adaptively change its visual servoing according to temporal body changes. We apply our method to a low-rigidity 6-axis arm, MyCobot, and confirm its effectiveness by conducting object grasping experiments based on visual servoing.

I. INTRODUCTION

Visual servoing is one of the most basic control strategies in robotics. It is usually applied to industrial robots that are highly rigid and have accurately calibrated vision and bodies [1], [2]. These methods often require carefully designed vision features and manually calibrated models. On the other hand, in addition to these general visual servoing methods, learning-based methods have been developed recently due to the advancement of deep learning [3]–[5]. There are two main types of learning methods: learning from demonstration [5], [6], in which a human teaches the movement, and reinforcement learning [3], [4], in which the control policy is learned from rewards through many trials in simulation. While the former is easy to apply to actual robots, it requires a lot of effort for human demonstration. The latter is based on learning in simulation, and is challenging to apply to robots that are difficult to modelize in simulation.

There are only few examples of applying visual servoing to low-rigidity robots whose bodies do not move as intended. In order to perform visual servoing on these low-rigidity robots, it is necessary to accurately modelize their flexible bodies and spend time on the calibration between vision and body [7], [8]. In addition, the body of a low-rigidity robot tends to change over time, which causes the model to change gradually, requiring multiple iterations of modeling and calibration [9]. Note that there are some examples of using a soft gripper for the hand of a rigid robot [10], but this is different from the focus of this study.

Based on these problems, we propose a method for a robot with a low rigidity and difficult-to-modelize body to learn its own law of visual servoing autonomously, taking into account temporal body changes (Fig. 1). The autonomous

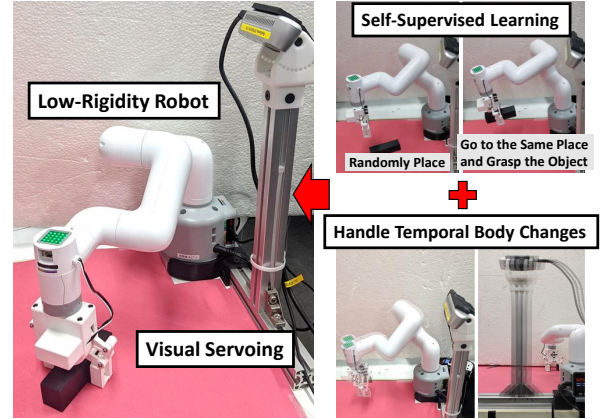


Fig. 1. The concept of this study: self-supervised learning of visual servoing and handling of temporal body changes for low-rigidity robots.

data collection is achieved not by human demonstration or reinforcement learning, but by repeatedly placing and picking up an object by itself. This is based on the fact that while it is difficult for the robot to directly grasp an object by visual recognition, it can grasp an object by reaching out to the exact same place if the object had been placed by itself. There is a similar data collection method [11], but it focuses only on automatic data collection for a rigid robot, and its goal is different from this study, which utilizes the motion reproducibility of a low-rigidity robot. Although our data collection method is limited to pick-and-place tasks, it is a basic motion common to various tasks, and we believe that it would be useful for cost effective robot that cannot move accurately due to low rigidity to learn such tasks autonomously. For adaptation to temporal body changes, we introduce parametric bias [12] and the robot adapts to the current body state by online learning of this variable. Parametric bias is a learnable input variable that has been mainly used for imitation learning in the field of cognitive robotics [13], [14], which we apply to visual servoing in this study. Changes in the dynamics of the model due to changes in the body over time, which are significant in a low-rigidity body, are implicitly embedded in this parametric bias, and the model adapts to the current state by constantly updating this variable to match the prediction of the vision sensor with the actual measured data. This study is useful and versatile in that it does not depend on a specific robot body structure and allows learning of visual servoing autonomously. Also, autonomous data collection mainly deals with the low-rigidity body of the robot, while parametric bias deals with

¹ The authors are with the Department of Mechano-Informatics, Graduate School of Information Science and Technology, The University of Tokyo, 7-3-1 Hongo, Bunkyo-ku, Tokyo, 113-8656, Japan. [kawaharazuka, kanazawa, k-okada, inaba]@jsk.t.u-tokyo.ac.jp

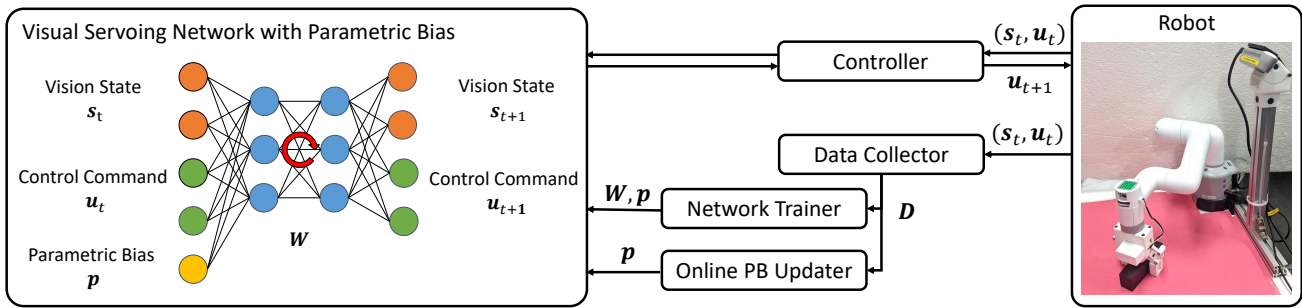


Fig. 2. The overall system of visual servoing network with parametric bias.

the temporal changes of the body. Therefore, it is possible to apply these two methods separately, for example, to low-rigidity robots without temporal body changes, high-rigidity robots with temporal body changes, etc.

The contributions of this study are as follows.

- Data collection for autonomous learning of a visual servoing model for a low-rigidity robot.
- Recognition and adaptation to changes in the visual servoing model due to temporal body changes.
- Acquisition of an object grasping controller by the actual robot with a low rigidity

The structure of this study is as follows. In Section II, we describe the network structure, data collection, network training, adaptation to the current body state, and visual servoing control, in order. In Section III, we describe data collection for a low-rigidity robot, online learning of parametric bias, and visual servoing experiments. We discuss the experimental results in Section IV and conclude in Section V.

II. SELF-SUPERVISED LEARNING OF VISUAL SERVOING CONSIDERING TEMPORAL BODY CHANGES

The overall system of this study is shown in Fig. 2. The network proposed in this study is called Visual Servoing Network with Parametric Bias (VSNPB).

A. Network Structure of VSNPB

The network structure of VSNPB can be expressed by the following equation,

$$(s_{t+1}, u_{t+1}) = h(s_t, u_t, p) \quad (1)$$

where t is the current time step, s is the visual information of the robot, u is the robot control input, p is the parametric bias (PB), and h is the visual servoing model. In this study, s is the vector z where image I_t is compressed by AutoEncoder [15]. Also, u is the target joint angle of the robot θ^{ref} . This varies depending on the robot, and for other robots such as tendon-driven robots, the target muscle length l^{ref} can be used for s [16]. Parametric bias p is a learnable input variable, and by collecting data while changing the body state in various ways, it is possible to embed the change in dynamics of h due to temporal body changes into p . Note that parametric bias can only handle static body changes, not dynamic ones.

In this study, VSNPB has ten layers, consisting of four FC layers (fully-connected layers), two LSTM layers (long short-term memory layers [17]), and four FC layers, in order. The number of units is set to $\{N_s + N_u + N_p, 300, 150, 50, 50$ (number of units in LSTM), 50 (number of units in LSTM), $50, 150, 300, N_s + N_u\}$ (where $N_{\{s,u,p\}}$ is the dimensionality of $\{s, u, p\}$). The activation function is Hyperbolic Tangent and the update rule is Adam [18]. Note that the input and output of the network are normalized using all the collected data. Regarding image compression, for a color image of 128×96 , convolutional layers with kernel size of 3 and stride of 2 are applied five times, the dimensionality is reduced stepwise to 256 and 15 units by two fully-connected layers, and then the image is reconstructed by fully-connected layers and deconvolutional layers in the same way. Batch Normalization [19] is applied to all layers except the last layer, the activation function is ReLU [20] for all layers except the last layer (where Sigmoid is used), and the update rule is Adam [18]. p is two-dimensional and the execution period of Eq. 1 is set to 1 Hz.

As for the dimension of PB, if it is too large, the space of PB is not self-organized well, and if it is too small, it becomes difficult to consider the temporal body changes. In general, it is preferable to set the dimension of PB to be slightly smaller than the dimension of possible changes. Even if there are many factors of temporal body changes, setting PB to a smaller dimension allows us to consider body changes better than if PB is not included, and similar body changes are compactly embedded in the same dimension.

B. Data Collection

In this study, we describe the data collection necessary for learning visual servoing autonomously. A low-rigidity robot cannot grasp an object simply by recognizing it and reaching for it as intended due to the nature of the robot. On the other hand, if the motion itself is reproducible, the robot can reach to the exact same position as before, when the trajectory of the joint angle is the same. The data collection in this study takes advantage of this feature, and the procedure is shown below.

- (1) Set the robot to the initial posture.
- (2) Have the robot hand grasp the target object in the desired way.

- (3) Have the robot reach out to a random position and release the object to return to the initial posture.
- (4) Have the robot reach out to the exact same position as before using the same procedure as in (3), grasp the object, and return to the initial posture.
- (5) Repeat (3) and (4) until the data collection is complete, then return to (1) and repeat the process of grasping another object.

We need to reflect the desired angle and position of the grasp in (2) because this grasping configuration will always be used during the data collection. In (3), various motion trajectories are considered, and the robot is moved by the same procedure in (4), so if there is a specific speed of the robot or some specific motions such as pregrasp are required, they should be included here. In order to ensure the reproducibility of the robot motion in (4), it is very important to follow the exact same procedure as in (3). In particular, if there are dynamic elements in the motion, the robot may reach to different places if the speed of the motion is not kept the same. On the other hand, if there is reproducibility, procedures (3) and (4) will always succeed, and the robot can continue to collect data autonomously. In this way, it is possible to collect a time series of data as if the robot is executing feedback control of its body to the target object using its vision.

C. Training of VSNPB

Using the obtained data D , we train VSNPB. In this process, by collecting data while changing the body state, we can implicitly embed this information into the parametric bias. When taking into account the changes in the body due to aging, data should be collected for each degree of aging. The data collected for the same body state k can be expressed as $D_k = \{(s_1, \mathbf{u}_1), (s_2, \mathbf{u}_2), \dots, (s_{T_k}, \mathbf{u}_{T_k})\}$ ($1 \leq k \leq K$, where K is the total number of body states and T_k is the number of motion steps for the trial in the body state k), and the data used for training $D_{train} = \{(D_1, \mathbf{p}_1), (D_2, \mathbf{p}_2), \dots, (D_K, \mathbf{p}_K)\}$ is obtained. Here, \mathbf{p}_k is the parametric bias that represents the dynamics in the body state k , which is a common variable for that state and a different variable for another state. Using this D_{train} , VSNPB is trained. In usual learning processes, only the network weight W is updated, but here, W and \mathbf{p}_k for each state are updated simultaneously. In this way, \mathbf{p}_k embeds the difference of dynamics in each body state. The mean squared error for s and \mathbf{u} is used as the loss function in the training, and all \mathbf{p}_k are optimized with $\mathbf{0}$ as initial values.

D. Online Update of Parametric Bias

Using the data D obtained in the current body state, we update the parametric bias online. If the network weight W is updated, VSNPB may overfit to the data, but if only the low-dimensional parametric bias \mathbf{p} is updated, no overfitting occurs. This online learning allows us to obtain a model that is always adapted to the current body state.

Let the number of data obtained be $N_{data}^{nonline}$, and start online learning when the number of data exceeds $N_{thre}^{nonline}$. For each new data, we set the number of batches as $N_{batch}^{nonline}$, the number

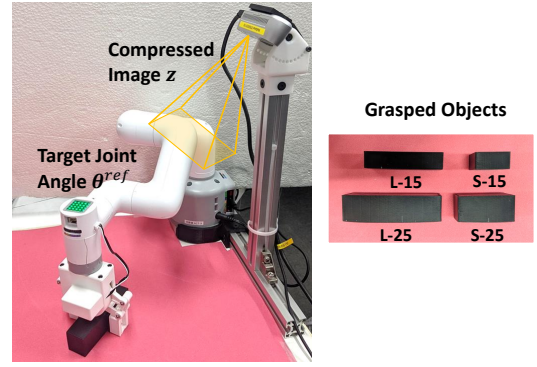


Fig. 3. The experimental setup of the low-rigidity robot MyCobot and four grasped objects.

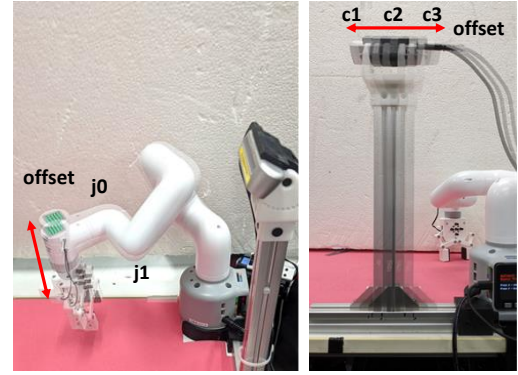


Fig. 4. The temporal body changes handled in this study: change in realization of joint angle and change in camera position.

of epochs as $N_{epoch}^{nonline}$, and the update rule as MomentumSGD. For the loss function, we use the mean squared error for s only. It is also important to note that W is fixed and only \mathbf{p} is updated. Data exceeding $N_{max}^{nonline}$ are deleted from the oldest ones.

E. Visual Servoing Using VSNPB

Visual servoing using VSNPB is very simple. We only need to calculate the control input \mathbf{u}_{t+1} at the next time step by forward propagation from the current visual state s_t and the control input \mathbf{u}_t . In this case, W is obtained from Section II-C and \mathbf{p} is obtained from Section II-D.

III. EXPERIMENTS

A. Experimental Setup

The experimental setup of this study is shown in Fig. 3. The robot used in this study is MyCobot, whose body is made of plastic and whose links flex and joints easily change due to loosening of screws. The camera is RealSense D435. s is the color image compressed by AutoEncoder z , and \mathbf{u} is the target joint angle θ^{ref} . Here, θ^{ref} is 7-dimensional, which are the dimensions of the six joints of the robot and the opening and closing of the gripper (0 when open and 1 when closed). When \mathbf{u} calculated in Section II-E is sent to the robot, the gripper is closed if the value is more than 0.5, and open otherwise. In this study, we use four objects

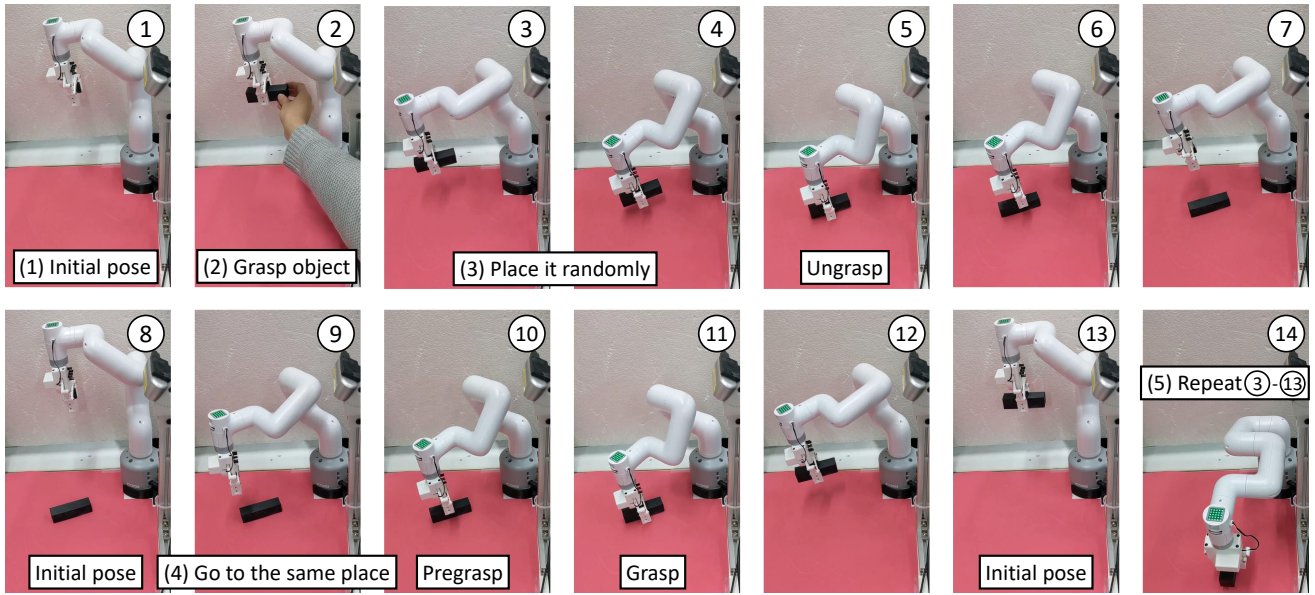


Fig. 5. The procedure of data collection for visual servoing.

of different lengths (L or S) and widths (15 mm or 25 mm), denoted L-15, S-15, L-25 and S-25, as shown in Fig. 3. Note that the maximum opening of the gripper is 38 mm.

For temporal body changes, we handle the change in the realization of the joint angle and the change in the camera position, as shown in Fig. 4. This is because the two main aging factors of the low-rigidity robot handled in this study are the misalignment of the origin of joints due to loosening of screws and the misalignment of the camera and the robot due to reassembling of the robot. Our experimental setup simply imitates these factors. Although it would be desirable to directly handle the temporal changes in the body state while the robot is moving for a long period of time, it is difficult to evaluate the changes quantitatively, so the changes in the body state are virtually created in this study. For the realization of the joint angle, we prepare two states, j_0 and j_1 , where j_0 is the case that θ^{ref} is directly sent to the robot and j_1 is the case that an offset of 2 deg is added to the target angles of all joints. For the change of the camera position, c_1 , c_2 , and c_3 are prepared, and the camera position is offset by 10 mm each. Note that it is not necessary to know these offset values in the training of VSNPB, so it is possible to embed body changes that are difficult to explicitly parameterize into PB.

B. Data Collection and Training Experiment

The data collection process is shown in Fig. 5. Note that (1)–(5) in Fig. 5 denotes the numbers in Section II-B, and ①–⑭ denotes the image numbers. First, we set an initial posture and let the robot grasp an object in the desired way. The robot places the object at a random position within the range where inverse kinematics can be solved. In this case, it is necessary to reflect the desired motion during the actual grasping task to the object placement motion. In this study, we define the state of pregrasp at ④, the robot

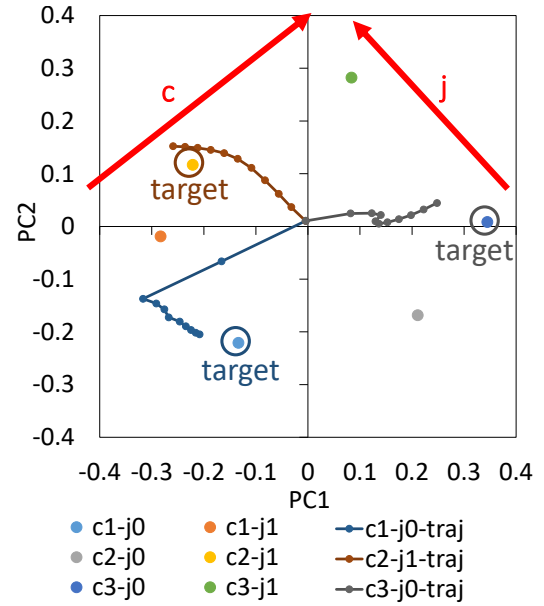


Fig. 6. The trained parametric bias and its trajectory when conducting online update of parametric bias at c_1-j_0 , c_2-j_1 , and c_3-j_0 .

moves quickly to this point, and then slowly lowers the hand to this point to ⑤ to open the gripper. The robot then returns to the pregrasp state in the same manner at ⑥, and from there returns to the initial posture. Next, the steps from ③ to ⑧ are performed in exactly the same manner except for the opening and closing of the gripper. The robot reaches its hand out to the exact same place as in ⑤, makes the pregrasp posture at ⑩, grasps the object at ⑪, and returns to the initial posture. By repeating this procedure many times, it is possible for the robot to autonomously collect data.

In this study, we train VSNPB by collecting data while changing the body state into six different states and perform-

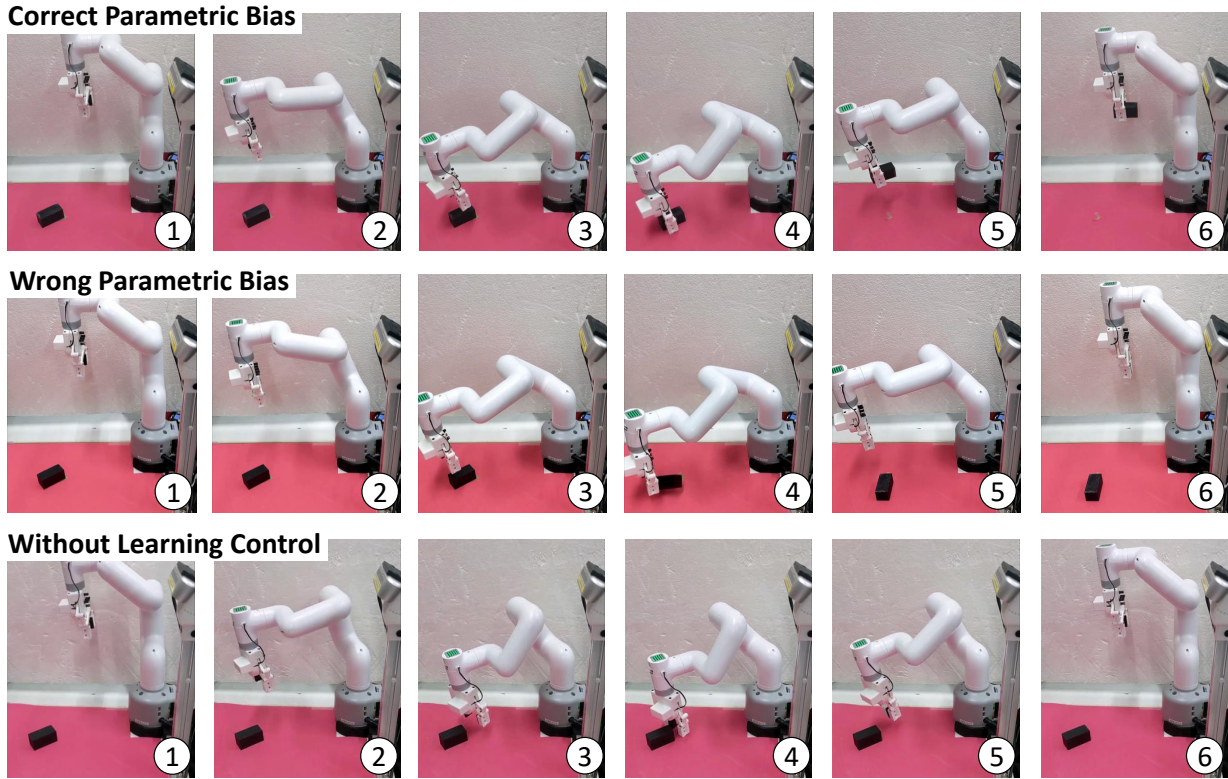


Fig. 7. The experiment of visual servoing with correct or wrong parametric bias, or without any learning control.

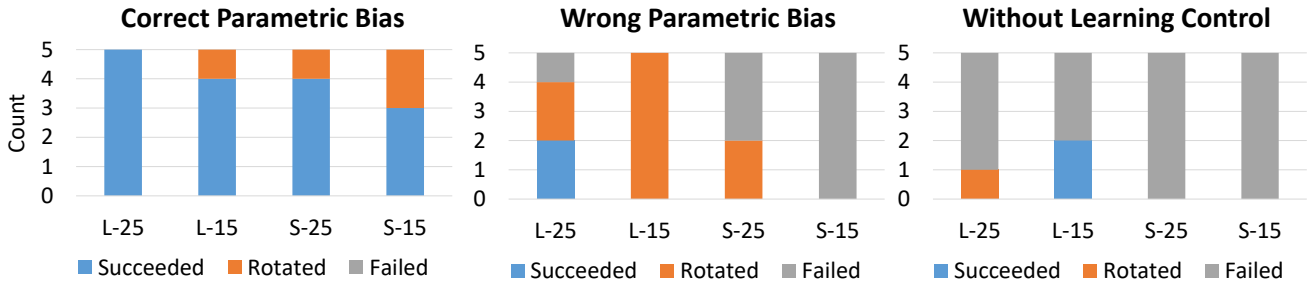


Fig. 8. The ratio of Succeeded, Rotated, and Failed when conducting visual servoing with correct or wrong parametric bias, or without any learning control.

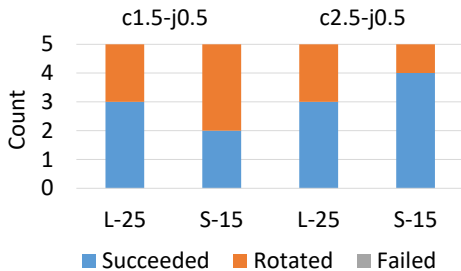


Fig. 9. The ratio of Succeeded, Rotated, and Failed when conducting visual servoing with untrained body state and after online learning of PB.

ing 30 trials for each of the four types of objects (five trials for each body state), totaling 120 trials. Parametric bias p_k trained in this process is shown in Fig. 6. We can see that

the parametric bias is regularly self-organized along the axes of $\{c1, c2, c3\}$ and $\{j0, j1\}$.

We also conducted an experiment in which the body state is set to $\{c1-j0, c2-j1, c3-j0\}$ and the control in Section II-E is conducted while the online update in Section II-D is performed simultaneously. The trajectory of the parametric bias p is shown as “-traj” in Fig. 6. It is found that the current parametric bias gradually approaches the parametric bias trained in the current body state, and that it is possible to accurately recognize the current body state from the prediction error of the sensors during the motion.

C. Visual Servoing Experiment

The experimental results of the actual visual servoing are shown in Fig. 7 and Fig. 8. Four objects are placed at different positions and are grasped five times each by

visual servoing. Here, "Succeeded" means that the robot succeeded in grasping the object, "Rotated" means that the robot succeeded in grasping the object but the gripper hit the edge and the object rotated, and "Failed" means that the robot failed to grasp the object. In all experiments, the body state is set to $c2-j0$, and we compare the case where the correct parametric bias trained for the same state is used (Correct) with the case where the wrong parametric bias trained for the state $c3-j1$ is used (Wrong). We also compare a general object grasping method that does not use VSNPB, such as detecting a tabletop object using plane detection and euclidean clustering, and solving inverse kinematics to it. Here, we use a rigid body approximation of the robot and the camera position on CAD (although it is possible to tune the robot and camera model over time, we use the geometric model as it is to show the control error of the low-rigidity robot). Fig. 7 shows examples of motions for the object S-25. The motion depends on the value of PB, and it can be seen that the robot correctly grasps the object when the value of PB is Correct, while it fails when the value of PB is Wrong. In the case without the learning control, the hand is greatly displaced and does not even touch the object. In Fig. 8, we show the success rate for each object. In the case of Correct, all grasplings Succeeded or Rotated, while in the case of Wrong, the probability of failure increases. This signifies that the recognition of the current body state is important. In both cases, the larger the object is, the higher the success rate of the grasping is. In the case of a small object, a small deviation often causes a failure of the grasp. When the learning control is not used, the grasping fails in most cases due to model errors. Some of the grasping is considered to be successful, but this is only the case when the robot can just barely grasp the edge of a long object.

Finally, regarding the body states that were not used during the training, the results of the same experiment as above for L-25 and S-15 are shown in Fig. 9 after the online update of PB. Here, the experiments are conducted for the cases where the body state is set as a combination of the following: $c1.5$ between $c1$ and $c2$ or $c2.5$ between $c2$ and $c3$ for the camera position, and $j0.5$ between $j0$ and $j1$ for the realization of joint angles, i.e. $c1.5-j0.5$ and $c2.5-j0.5$. The results show that the success rates for both cases are higher than those of Wrong cases in Fig. 8, and not much different from those of Correct cases. We can see that even the body states that were not used in the training can be estimated by updating PB, and the visual servoing can be executed appropriately according to the body state.

IV. DISCUSSION

We discuss the results of our experiments. First, regarding data collection, we found that even a low-rigidity robot can autonomously collect data by using the reproducibility of its own body movements. On the other hand, there are a few parts that are not reproducible. If we want to perform 10 trials, there is no problem, but in order to perform 100 trials, a manual adjustment of the grasping position of the object is necessary halfway through the trials. Next, in

the training of VSNPB, the parametric bias self-organizes regularly along the body state change. In addition, online learning enables us to recognize the current body state accurately. Finally, for the actual visual servoing, though the success rate varies depending on the size of the object, the grasping is successful with a high probability if the body state is correctly recognized. Even if the body state is not given as data for training, it is possible to perform the grasping accurately by combining with the online update of PB. On the other hand, the failure rate of grasping increases when the body state is not recognized well, and there are many cases where the robot cannot even touch the object without the learning control.

A major advantage of this study is the autonomy of the robot to collect data by itself. In addition, for example, if data is collected for each state in a robot whose screws are gradually loosening, it will be possible to accurately handle the body state of the robot both when the screws are tightened and when they are loosened. It is also important to note that we do not need to reproduce a low-rigidity body in a simulation, nor do humans need to teach the robot how to move. Also, as this study does not assume a specific body structure, it can be applied to a variety of robots such as musculoskeletal humanoids [16] or flexible octopus-like robots [21] in the future. In this study, we chose simple rectangular objects as objects to be grasped to emphasize the concept of the method, but we believe that we can show the advantages of this learning control further by applying it to more complex objects.

Finally, we discuss the limitations of this study. First, our system assumes that the object is placed on a flat surface when it is randomly placed, and that the robot can grasp the object if it behaves exactly as it did when placing the object. Therefore, if the environment in which the objects are placed is complex and the position and angle of the object changes at the moment of placing the object, the robot cannot grasp the object even if it reaches to the same place. Secondly, this study does not deal with multiple objects, and this problem also needs to be solved. For this, we need to label the objects to be grasped in the network input, or use implicit expressions as in Implicit Behavior Cloning [22].

V. CONCLUSION

In this study, we proposed a deep learning model to handle automatic data collection and temporal body changes, which are problematic when a low-rigidity robot performs visual servoing. For data collection, we proposed a method where the robot autonomously collects data by repeatedly placing an object and reaching out to the same place by itself, taking advantage of the fact that the low-rigidity robot has difficulty performing the intended movement but has reproducibility in motion. For the temporal body changes, we introduced parametric bias, which can embed the implicit changes in dynamics into the model, and proposed a method for the robot to adapt to its current body state by updating the parametric bias to match the current prediction and the actual measurement. We applied this method to an actual robot with

low-rigidity, and confirmed its effectiveness for a grasping task for several objects with various positions and angles. In the future, we would like to construct a system that can autonomously learn the relationship between body sensors and motions even for low-rigidity, flexible, and complex robots, taking into account multiple target objects and various ways of grasping.

REFERENCES

- [1] Y. Shirai and H. Inoue, "Guiding a robot by visual feedback in assembling tasks," *Pattern Recognition*, vol. 5, no. 2, pp. 99–108, 1973.
- [2] B. Espiau, F. Chaumette, and P. Rives, "A new approach to visual servoing in robotics," *IEEE Transactions on Robotics and Automation*, vol. 8, no. 3, pp. 313–326, 1992.
- [3] T. Lampe and M. Riedmiller, "Acquiring visual servoing reaching and grasping skills using neural reinforcement learning," in *Proceedings of the 2013 International Joint Conference on Neural Networks*, 2013, pp. 1–8.
- [4] A. X. Lee, S. Levine, and P. Abbeel, "Learning Visual Servoing with Deep Features and Fitted Q-Iteration," in *Proceedings of the 5th International Conference on Learning Representations*, 2017, pp. 1–20.
- [5] T. Zhang, Z. McCarthy, O. Jow, D. Lee, X. Chen, K. Goldberg, and P. Abbeel, "Deep Imitation Learning for Complex Manipulation Tasks from Virtual Reality Teleoperation," in *Proceedings of the 2018 IEEE International Conference on Robotics and Automation*, 2018, pp. 5628–5635.
- [6] N. Saito, T. Ogata, S. Funabashi, H. Mori, and S. Sugano, "How to Select and Use Tools? : Active Perception of Target Objects Using Multimodal Deep Learning," *IEEE Robotics and Automation Letters*, vol. 6, no. 2, pp. 2517–2524, 2021.
- [7] H. Wang, B. Yang, Y. Liu, W. Chen, X. Liang, and R. Pfeifer, "Visual Servoing of Soft Robot Manipulator in Constrained Environments With an Adaptive Controller," *IEEE/ASME Transactions on Mechatronics*, vol. 22, no. 1, pp. 41–50, 2017.
- [8] P. Chatelain, A. Krupa, and N. Navab, "3D ultrasound-guided robotic steering of a flexible needle via visual servoing," in *Proceedings of the 2015 IEEE International Conference on Robotics and Automation*, 2015, pp. 2250–2255.
- [9] K. Kawaharazuka, K. Tsuzuki, M. Onitsuka, Y. Asano, K. Okada, K. Kawasaki, and M. Inaba, "Object Recognition, Dynamic Contact Simulation, Detection, and Control of the Flexible Musculoskeletal Hand Using a Recurrent Neural Network With Parametric Bias," *IEEE Robotics and Automation Letters*, vol. 5, no. 3, pp. 4580–4587, 2020.
- [10] C. Choi, W. Schwarting, J. DelPreto, and D. Rus, "Learning Object Grasping for Soft Robot Hands," *IEEE Robotics and Automation Letters*, vol. 3, no. 3, pp. 2370–2377, 2018.
- [11] M. Kanamura, K. Suzuki, Y. Suga, and T. Ogata, "Development of a Basic Educational Kit for Robotic System with Deep Neural Networks," *Sensors*, vol. 21, no. 11, pp. 1–21, 2021.
- [12] J. Tani, "Self-organization of behavioral primitives as multiple attractor dynamics: a robot experiment," in *Proceedings of the 2002 International Joint Conference on Neural Networks*, 2002, pp. 489–494.
- [13] T. Ogata, H. Ohba, J. Tani, K. Komatani, and H. G. Okuno, "Extracting multi-modal dynamics of objects using RNNPB," in *Proceedings of the 2005 IEEE/RSJ International Conference on Intelligent Robots and Systems*, 2005, pp. 966–971.
- [14] R. Yokoya, T. Ogata, J. Tani, K. Komatani, and H. G. Okuno, "Experience Based Imitation Using RNNPB," in *Proceedings of the 2006 IEEE/RSJ International Conference on Intelligent Robots and Systems*, 2006, pp. 3669–3674.
- [15] G. E. Hinton and R. R. Salakhutdinov, "Reducing the Dimensionality of Data with Neural Networks," *Science*, vol. 313, no. 5786, pp. 504–507, 2006.
- [16] K. Kawaharazuka, S. Makino, K. Tsuzuki, M. Onitsuka, Y. Nagamatsu, K. Shinjo, T. Makabe, Y. Asano, K. Okada, K. Kawasaki, and M. Inaba, "Component Modularized Design of Musculoskeletal Humanoid Platform Musashi to Investigate Learning Control Systems," in *Proceedings of the 2019 IEEE/RSJ International Conference on Intelligent Robots and Systems*, 2019, pp. 7294–7301.
- [17] S. Hochreiter and J. Schmidhuber, "Long short-term memory," *Neural computation*, vol. 9, no. 8, pp. 1735–1780, 1997.
- [18] D. P. Kingma and J. Ba, "Adam: A Method for Stochastic Optimization," in *Proceedings of the 3rd International Conference on Learning Representations*, 2015, pp. 1–15.
- [19] S. Ioffe and C. Szegedy, "Batch Normalization: Accelerating Deep Network Training by Reducing Internal Covariate Shift," in *Proceedings of the 32nd International Conference on Machine Learning*, 2015, pp. 448–456.
- [20] V. Nair and G. E. Hinton, "Rectified Linear Units Improve Restricted Boltzmann Machines," in *Proceedings of the 27th International Conference on Machine Learning*, 2010, pp. 807–814.
- [21] C. Laschi, M. Cianchetti, B. Mazzolai, L. Margheri, M. Follador, and P. Dario, "Soft Robot Arm Inspired by the Octopus," *Advanced Robotics*, vol. 26, no. 7, pp. 709–727, 2012.
- [22] P. Florence, C. Lynch, A. Zeng, O. Ramirez, A. Wahid, L. Downs, A. Wong, J. Lee, I. Mordatch, and J. Tompson, "Implicit Behavioral Cloning," in *Proceedings of the 2021 Conference on Robot Learning*, 2021.